Atmos. Chem. Phys., 8, 6551–6563, 2008
www.atmos-chem-phys.net/8/6551/2008/

Atmospheric Chemistry and Physics

Diurnal variations in the UV albedo of arctic snow

O. Meinander[1], **A. Kontu**[1], **K. Lakkala**[1], **A. Heikkilä**[1], **L. Ylianttila**[2], **and M. Toikka**[3]

[1]Finnish Meteorological Institute, P.O. BOX 503, 00101 Helsinki, Finland
[2]Radiation and Nuclear Safety Authority, P.O. Box 14, 00881 Helsinki, Finland
[3]Toikka Engineering Ltd., Hannuntie 18, 02360 Espoo, Finland

Received: 3 January 2008 – Published in Atmos. Chem. Phys. Discuss.: 29 February 2008
Revised: 2 September 2008 – Accepted: 23 September 2008 – Published: 14 November 2008

Abstract. The relevance of snow for climate studies is based on its physical properties, such as high surface reflectivity. Surface ultraviolet (UV) albedo is an essential parameter for various applications based on radiative transfer modeling. Here, new continuous measurements of the local UV albedo of natural Arctic snow were made at Sodankylä (67°22′N, 26°39′E, 179 m a.s.l.) during the spring of 2007. The data were logged at 1-min intervals. The accumulation of snow was up to 68 cm. The surface layer thickness varied from 0.5 to 35 cm with the snow grain size between 0.2 and 2.5 mm. The midday erythemally weighted UV albedo ranged from 0.6 to 0.8 in the accumulation period, and from 0.5 to 0.7 during melting. During the snow melt period, under cases of an almost clear sky and variable cloudiness, an unexpected diurnal decrease of 0.05 in albedo soon after midday, and recovery thereafter, was detected. This diurnal decrease in albedo was found to be asymmetric with respect to solar midday, thus indicating a change in the properties of the snow. Independent UV albedo results with two different types of instruments confirm these findings. The measured temperature of the snow surface was below 0°C on the following mornings. Hence, the reversible diurnal change, evident for ∼1–2 h, could be explained by the daily metamorphosis of the surface of the snowpack, in which the temperature of the surface increases, melting some of the snow to liquid water, after which the surface freezes again.

Correspondence to: O. Meinander
(outi.meinander@fmi.fi)

1 Introduction

The relevance of snow for climate variability and change is based on its physical properties, such as high surface reflectivity, i.e., albedo (IPCC, 2007). High albedo has an important influence on the surface energy budget and on Earth's radiative balance (Forster et al., 2007, e.g.). Snow albedo varies with wavelength, and therefore the strength of the feedback depends on a number of factors, such as the depth and age of the snow cover, and the amount of incoming solar radiation and cloud cover. The albedo of snow may decrease because of anthropogenic soot (Wiscombe and Warren, 1980; Warren and Wiscombe, 1980) and aging and melting (Wiscombe and Warren, 1980; Blumthaler and Ambach, 1988; Wuttke et al., 2006). In the melting process, often initiated in springtime by the increase of shortwave irradiance, the snow grains are filled with liquid water and the density of the snow may increase, e.g., in the open sites of Arctic Finland, to 350 kg/m^3 (Kuusisto, 1984). When the albedo decreases, more radiation is absorbed, and the melting of the snow may increase due to this albedo feedback mechanism (e.g., Bony et al., 2006). In addition to its climate connections, ultraviolet radiation (UV) reflected from snow and ice may cause unprotected eyes the painful condition of snow blindness (UNEP, 2002). The UV albedo for a surface with snow is high, and also due to multiple reflections affects downwelling radiation (Bais and Lubin, 2007). Snow cover can increase erythemal irradiance by up to 60% compared to a snow-free case (Weatherhead et al., 2005, e.g.). Moreover, surface UV albedo is an essential parameter for various applications based on radiative transfer (RT) modeling, including various satellite retrieval algorithms. For example, current satellite UV algorithms demand better information on UV albedo, especially for land when covered by snow (e.g., Arola et al., 2003, Tanskanen and Manninen, 2007).

Published by Copernicus Publications on behalf of the European Geosciences Union.

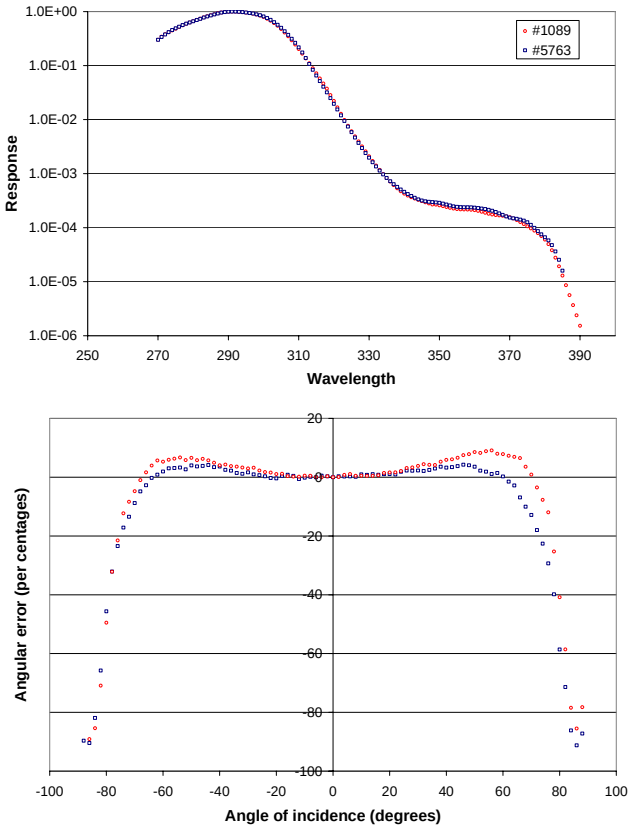

Fig. 1. Spectral (above) and cosine (below) responses of the SL501 sensors. Spectral responses are in logaritmic scale showing the maximal differences. The responses of the upward and downward sensors need to be considered when albedo results are interpreted.

Accurate ground-based long-term albedo measurements of snow are somewhat sparse due to the harsh conditions with snow. Broadband albedo, measured with pyranometers, has been more widely studied (Pirazzini, 2004; Pirazzini et al., 2006; Wuttke et al., 2006), and spectral studies are less (Perovich et al., 2002; Wuttke et al., 2006). Only a few studies on UV albedo of snow have been published, some of them for Antarctic (e.g., Smolskaia et al, 1999; Wuttke, et al., 2006) and few for Arctic snow (e.g., Perovich et al, 2002), and moreover, most of them are campaigns, not continuous high temporal resolution measurements. As far as albedo is concerned, Arctic and Antarctic snow differ from each other especially in two ways: Antarctic snow has smaller snow grain sizes, and has more pure snow unaffected by impurities. Grain sizes of up to approx. 3 mm have been reported for the Arctic snow (Pirazzini et al., 2006). For these reasons, a lower albedo is expected for Arctic snow.

On the basis of earlier studies by others, it was our hypothesis that snow melt will decrease the UV albedo of Arctic snow. Moreover, it was our goal to study, using continuous high temporal resolution 1-min measurements over the whole melt season, how the decrease actually happens: in a single dramatic change, step-by-step or decreasing more or less linearly, little by little. Also, our aim was to study how the temperature of the air and ground, grain size of the snow, and amount of snow, as well as incoming irradiance and cloudiness possibly affect the albedo. To avoid misinterpretation of the experimental data, the error sources have to be considered. A detailed analysis of the uncertainties in UV measurements is available in Bernhard and Seckmeyer (1999), and azimuthal errors in spectral UV data have been explained in Meinander et al. (2006). The effects of instrumental uncertainties, such as calibration and cosine error, atmospheric parameters, solar zenith angle, and geometric aspects, like slopes and shadows, are considered in Sects. 2 and 4, and discussed further in Sect. 5.

2 Materials and methods

2.1 UVB albedo measurements

New polar Arctic measurements on the local UV albedo of snow were planned and carried out in 2007 at Sodankylä, (67°22′N, 26°39′E, 179 m a.s.l.), Finland. For UV albedo measurements, two sensors of the UV Biometer Model 501 from Solar Light Co. (SL501) with similar spectral and cosine responses (Figs. 1 and 2) were used, one facing upwards and the other downwards at a height of 2 m. The SL501 spectral response resembles the action spectrum for erythema, wavelengths in the UVB (280–310 nm) being most weighted. For the albedo measurements, a fixed device for the setting-up and support of the two sensors, including independent leveling possibilities for the upward and downward SL501s, a blower to keep the sensors defrosted, and a data logger system, was planned and constructed at FMI (Fig. 2). Data were logged into the data base from 25 February (day 56) till 15 May (day 135) 2007 at 1-min-intervals. This period included various phases, including both the accumulation and melting of snow. The albedo of snow (A) was calculated from the ratio of downwelling UV irradiance on to upwelling irradiance ($UV_{ery}\uparrow/UV_{ery}\downarrow$) measured at 2π.

2.2 Multiband data

In order to gain wavelength-dependent snow albedo information, the reflected irradiance was also measured at 1-min intervals with an multibandfilter radiometer (MBFR, NILU-UV type), placed facing downwards close (3 m) to the SL501 albedo sensors. These multichannel measurements were made from 6 February (day 37) till end of May, 2007. In addition, one NILU-UV radiometer facing upwards was situated close by (30 m), on the roof of the Sodankylä Observatory. The NILU-UV radiometer measures UV in five channels with central wavelengths around 305, 312, 320, 340 and 380 nm, and bandwidths of around 10 nm at FWHM. A sixth channel measures photosynthetically active radiation (PAR) in the range of 400–700 nm. With these channels,

Table 1. The midday SZA values [degrees] (at accuracy of one degree) at Sodankylä (67°22′N, 26°39′E) in 2007, and the time for solar noon [UTC] (at accuracy of ten minutes).

Month	February		March		April		May
Date	1	15	1	15	1	15	1
Solar noon	10.30	10.30	10.30	10.20	10.20	10.20	10.10
SZA	85	80	75	70	63	58	53

UVA and UVB, and erythemally-weighted UV albedo can be calculated from the ratio of downwelling irradiance to upwelling irradiance, UVA↑/UVA↓, UVB↑/UVB↓, and UV_{ery}↑/UV_{ery}↓, measured at 2π. The characteristics of the instruments are described more in detail in Hoiskar et al. (2003).

2.3 Empirical calibration

The aim of this work was to have an understanding of this valuable empirical data set on albedo, measured under the hard conditions of Arctic snow, without introducing any additional uncertainties or errors to the data due to imperfect correction procedures, nor to let the uncertainties and errors in the original data to affect the final results.

During the winter months, the sun does not rise at all at Sodankylä. Even at the beginning of the measurement period in February, the sun is still very low. On 15 March (day 74) the midday SZA falls less than 70.0 degrees for the first time (Table 1). With an SZA larger than 70 degrees, the cosine error increases dramatically (Fig. 1), but as most of the irradiance is then diffuse (at 300 nm more than 90%, e.g. Madronich, 1993), this has only little impact on the measurement results. However, the amount of radiation reaching the Earth is then minimal (UVI<1), increasing the uncertainties in the measurements. On the other hand, during the measurement period, the midday SZA significantly decreases (SZA<55°, UVI>3) as the length of the day grows. To avoid misinterpretation of data, knowledge of the SZA is thus essential.

The optimum calibration of the raw signal requires calibration matrix with SZA and ozone (Webb et al., 2006):

$$E_{\mathrm{CIE}} = (U - U_{\mathrm{offset}}) \times C \times f_n(\mathrm{SZA}, \mathrm{TO_3}) \times \varepsilon(T) \times \mathrm{Coscor} \quad (1)$$

where E_{CIE} is the erythemal effective irradiance, U is the measured electrical signal from the radiometer, U_{offset} is the electrical offset for dark conditions, C is the calibration coefficient (a constant value determined for specific conditions like SZA=40° and O_3=300 DU), f_n is a function that can be expressed as a calibration matrix normalized at, e.g., SZA=40° and O_3=300 DU, $\varepsilon(T)$ is the temperature correction function, and Coscor is the cosine correction function.

The use of Eq. (1) will be discussed more in Sect. 5. Here, the calibration factors (C) of the sensors had been determined by the Finnish Radiation and Nucleation Safety Authority (STUK), before the albedo measurements (in 2005 and 2006), as an average for conditions with 38<SZA<60 degrees. The ratio of the calibration coefficients of the sensors was then C1/C2=1.13. After the albedo measurements, the calibration was carried out again, giving C1/C2=1.19. The sensor with the originally better response was installed to measure the upwelling reflected radiation.

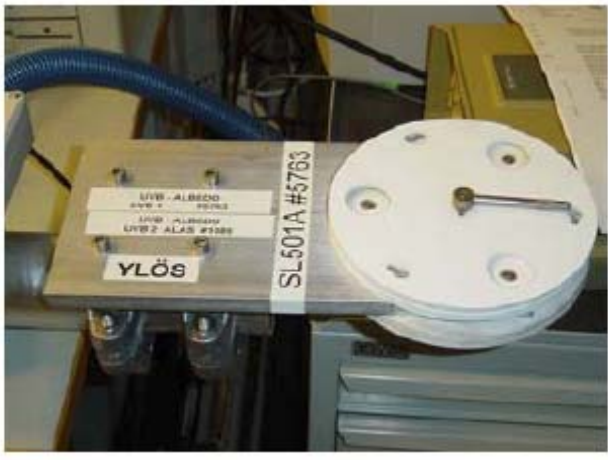

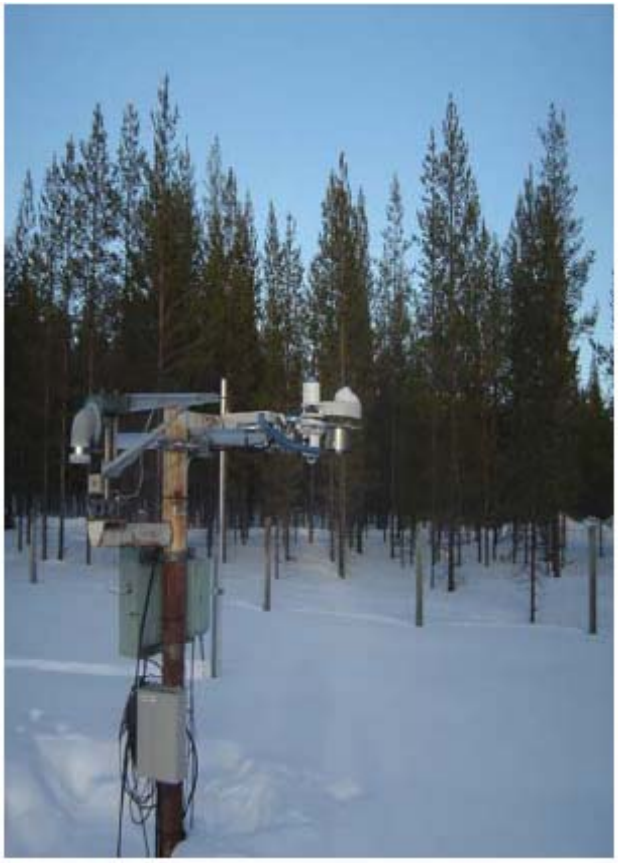

Fig. 2. The holders designed for the albedo measurements.

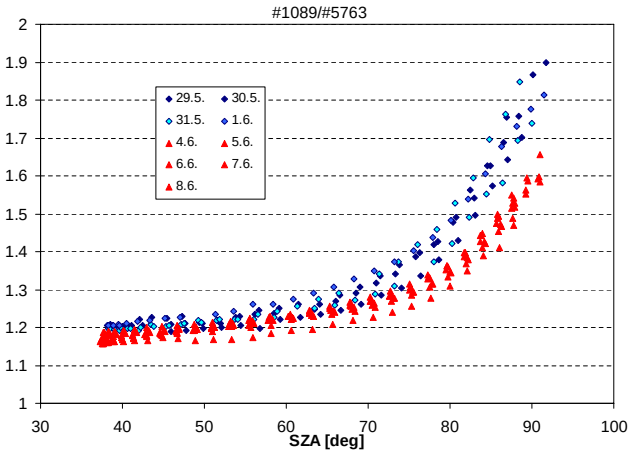

Fig. 3. Results of the post-calibration measurements of the SL501s in 2007.

Keeping in mind that i) the spectral responses of the sensors were measured to be similar (Fig. 1), and ii) the differences in the cosine responses were relatively small (Fig. 1), and iii) we are only interested in the relative signals of these two sensors, the calibration coefficients C1 and C2 might be sufficient for comparison of data representing a narrow SZA range, e.g., within 2–4 degrees. We also know that the upwelling irradiance measured by the SL501 is not as much affected by the cosine error, due to the missing direct component. The albedo derived from the SL501 data may therefore be an overestimation of the real albedo under a clear sky and high solar elevation angles, and uncertainties and errors minimize with increasing diffuse radiation under full cloudiness or lower sun.

However, due to the very low sun (SZA>60°), the use of the laboratory calibration as such was considered unsatisfactory. Several solutions existed: 1) New empirical calibration coefficients (c1 and c2) for the prevailing SZA conditions were produced on 27 March (day 86) by turning both of the sensors upwards and calibrating them against each other; both of them were also calibrated against an SL501 placed on the roof of the observatory. The sensors were again similarly calibrated on 2 May (day 122), and on 11 May (day 131) after snow melt. 2) The data of the prior and subsequent calibrations as a function of SZA were available. These data could be used to produce a simple SZA correction. 3) It would be possible to use a radiative transfer model to calculate the calibration as in Eq. (1).

Here, the empirical calibration approach was used. The aim was to produce empirically calibrated data with error estimates for the prevailing SZAs, without introducing any additional uncertainty or error in the data, due to a simplified SZA correction, as will be discussed more detailed in Sect. 5.

The empirical calibration factors were determined independently using two different SL501 sensors as references. First, the roof SL501 was used as a reference for both of the two albedo measurement sensors. Then, one of the albedo sensors was used as a reference for the other. In addition, empirical calibration procedures were carried out in May after the snow melt.

The empirical calibration factors c1 and c2 were calculated on the basis of the measurements (c1=1.09, c2=0.71 for March; c1=1.29, c2=0.96 for both cases in May). The ratio of the calibration factors in March was c1/c2=1.54 (SZA 67–69°). The ratio of the coefficients was the same whether the independent roof SL501 was used as a reference for both the sensors independently, or one of the two albedo SL501 sensors was used as a reference for the other. In May, the ratio was c1/c2=1.34 (SZA 56–60°). It seems that the ratio c1/c2 could possibly decline with the decline of SZA. The same fall in c1/c2 was evident when studying the data of the solar measurements made in 2007 by STUK for calibrating the same sensors (Fig. 3). It is possible, e.g., that the spectral response of one or both of the sensors had changed since its determination, as will be discussed more in Sect. 5. In any case, we can conclude that we have an SZA dependent-uncertainty in the data.

We can minimize or eliminate the SZA dependency effect by i) picking the corresponding SZA moments for each day, or ii) dividing albedo results into temporal subgroups based on SZA and snow conditions within which the daily variations are similar, and using the same empirical correction coefficient within the shorter period. Both of these approaches were used here, but the first was considered the better of the two, and was used for the more detailed studies for calculation of the empirically calibrated albedo A for SZA 56–60°:

$$A = \frac{c2\mathrm{UV_{ery}}\uparrow}{c1\mathrm{UV_{ery}}\downarrow} \quad (2)$$

where $c1$ and $c2$ are the empirically determined calibration factors for the SZA 56–60°, and $\mathrm{UV_{ery}}\uparrow$ and $\mathrm{UV_{ery}}\downarrow$ are the simultaneously measured upwelling and downwelling erythemally weighted irradiances.

The first occasion in 2007 on which a midday SZA<60° was achieved, for a period of at least one hour, was on 10 April (day 100). Hence, a continuous temporal data set including data measured with 56<SZA<60 degrees was obtained from 10 April until snow melting. These data were used as the core material for the current study.

The other subgroups used here for temporal data series, were based on SZA and snow, as follows: a) albedo during accumulation of snow in March and at the beginning of April with midday SZA>60° using the March empirical coefficients; b) albedo during the melting period from mid-April until snow melt and end of albedo measurements on 9 May (day 129) with midday SZA<60°. The difference caused by these subgroup calibration differences was also estimated by combining the data sets produced with different calibration coefficients. This comparison reveals the error which had been in the data, if there had been one empirical calibration

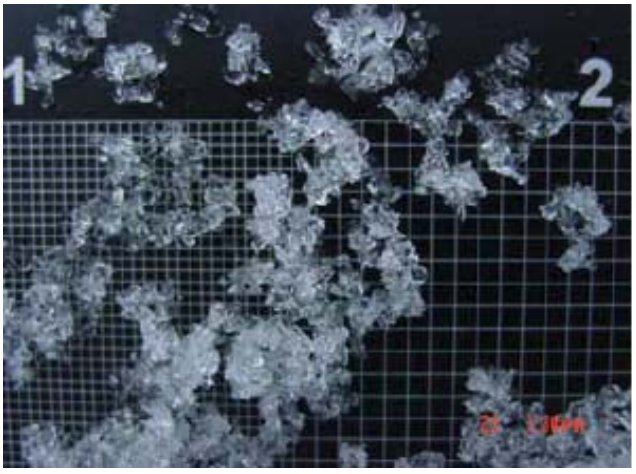

Fig. 4. The grids used for the snow grain size measurements. Numbers 1 and 2 in the figure indicate the corresponding grid sizes of 1 mm and 2 mm.

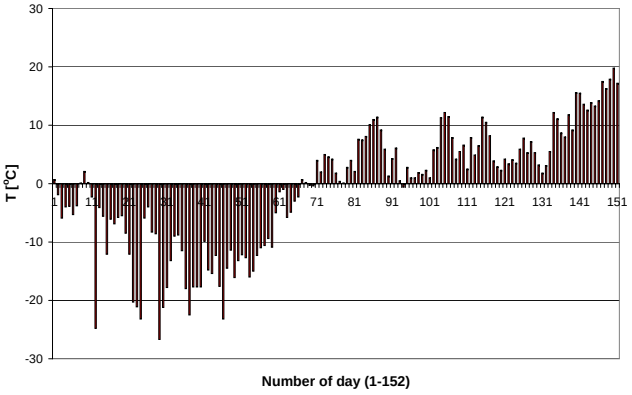

Fig. 5. The maximum air temperature T_{max} [°C] in 2007 showing the big jump, the "springthaw".

only, under too large SZA. These data were not used more in-depth studies but rather to understand the long-term variation of the albedo.

2.4 Ancillary data

At Sodankylä, the state of the atmosphere at a height of 2 m is measured once a minute by an automatic weather station (AWS). From these data, information on the beginning of rain, snow depth and cloud cover, e.g., can be gained.

Snow depth (h_s) and grain size (D) were measured at Sodankylä by one of the co-authors (A. Kontu) from November 2006 until 14 May 2007 (day 134), covering the whole albedo measurement period. The grain sizes of all the layers of snow were estimated visually regularly, approx. twice a week, by taking samples of snow on a screen with a mm-grid (Fig. 4). The sampling site was not exactly the same as that of the albedo measurements, but at a distance of 300 m under conditions that can be assumed to be similar. All other activities very close to the albedo measurement were forbidden; the diffusers were, however, cleaned if needed with as little disturbance to the surroundings as possible.

3 Ancillary results

3.1 Snow depth

In 2007, the maximum snow depth at Sodankylä was 68 cm, on 21 March (day 80) (Fig. 6). The second highest value of 67 cm occurred on the day before and the day after, but also on 12 April (day 102). After 12 April, the snow depth decreased monotonically until totally melted.

3.2 Temperature

On 7 March (day 66), the daily maximum air temperatures (Fig. 5) indicated a rapid jump, referred here as "a springthaw", from values below zero°C to values above zero. Neither the daily minimum temperatures nor the minimum temperature of the ground showed any similar rapid change.

Between 1 March–15 May (days 60–135), the measured minimum temperature of the ground at 06:00 UTC rose above 0°C on only six days. Otherwise the temperature remained below zero. From this it follows that, apart from these few cases, the snow surface was always frozen in the evening, night and early morning hours, lacking solar warming. On the other hand, the "springthaw" was not enough to start the snow melt alone, thus indicating the importance of radiation as the starting force for the snow melt.

3.3 Snow grain size

In the UV range of wavelengths, the reflected signal comes from the very surface, and only the surface layer grain size data were used here.

In 2007, the measured thickness of the surface layer varied from 0.5 to 35 cm. The surface layer snow grain size results can be divided into two groups: before and after 16 April (day 106) (Fig. 6). Before this date, the snow grain sizes were most often <0.5 mm. Thereafter, the grain size was most often from 1.0 to 2.5 mm, indicating the beginning of the actual snow melt period. However, there are no grain size results available between 10–16 April (days 100–106), and so the snow metamorphosis, with increasing grain size, began sometime within that period.

Grain size data was then studied to determine whether grain size had a relationship to temperature, snow depth and time (the day of the year). Such a relationship would mean that an albedo model could possibly predict Arctic snow UV albedo as a function of time (the day of the year) and temperature, rather than of grain diameter. Using the three variables

Fig. 6. Snow grain size D [mm] (dashed line with blue squares) and snow depth h_s [cm] (red solid line) in spring 2007.

Table 2. The correlation coefficient (r) of snow grain size and other measured parameters. The number of cases was n=17 between the days of 64–132.

Parameter	r
Minimum ground temperature	0.37
Daily maximum temperature	0.79
Grain size and time (number of day)	0.55
Depth of total snow pack	0.47
Depth of the surface layer	0.22

with the highest linear correlations (Table 2), the empirical relationship, giving an 82% explanation (r^2=0.82) for the Arctic snow grain size during the melting period was:

$$D = -0.04t + 0.19T\,\mathrm{max} - 0.03hs + 4.98 \quad (3)$$

where D is grain diameter, t is time (the day of the year) and Tmax is the daily maximum air temperature at a height of 2 m [°C] and hs is the height of the snowpack. The relationship between snow height and albedo is given in Eq. 4.

Even before the beginning of monotonical decrease in snow depth on 11 April (day 101), there were occasionally days with maximum air temperatures Tmax>0°C. On such days, e.g. on 26 and 29 March (days 85 and 88), the snow grain size was measured to be 2 mm.

4 UV albedo of snow

In addition to SZA information, the results were grouped according to cloudiness, as well as accumulation and melting of snow. We studied first the almost clear sky cases for SZA<60°, followed by cases of variable cloudiness, thereafter cases prior and after melt period, as well as averaged daily albedo during melting. Finally, long term variation in albedo was studied. The most important results were findings of an unexpected diurnal change in albedo during melting.

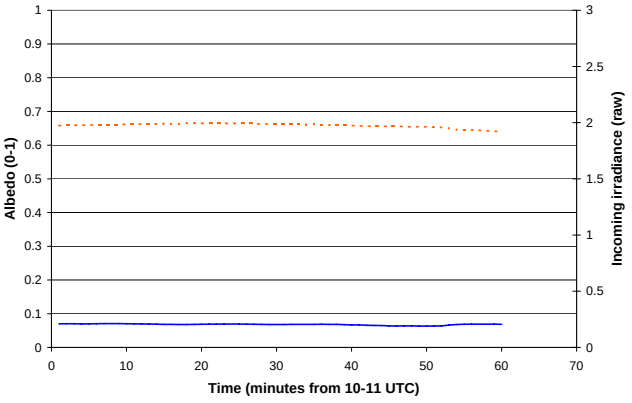

Fig. 7. Flat albedo signal (solid blue line) of a clear sky case (dashed orange line), 10 April (day 100) during the accumulation period.

An overview of the albedo results for SZA<60° in April is shown in Table 3. These results represent all cases of cloudiness. The minimum and maximum of the daily SL501 mean albedo, for SZA 56–60°, are included, indicating the diurnal changes. In some cases the results also suggested an asymmetric albedo, i.e. albedo decreasing from morning to afternoon. The results of the NILU-UV albedo are not included in Table 3, due to their use as complementary data for the current study.

4.1 UV albedo under almost cloudless sky

The signal of the upward sensor was used to study the cloudiness of the sky at exactly the same location and moment at which the albedo measurements were performed. For 56°<SZA<60°, i.e., from 10 April (day 100) onward, the almost-clear or clear-sky cases in April were: the 10, 15, 18, and 22 April (days 100, 105, 108, 112) (Table 3). Of these four cases, the first one occurred at the end of the snow accumulation period, and the last three during the melting season.

4.1.1 Stable albedo during accumulation period

The first case, 10 April (day 100), was an almost clear day during the snow accumulation period. The snow UVB albedo at midday was from 0.64 to 0.66 (Fig. 7), slightly increasing as the sun reached its highest elevation. The slight variation in the incoming irradiance had no effect on the albedo. Similarily, the NILU-UV albedo showed stable UVA and UVB reflectance. The surface layer snow grain size was small, 0.3 mm. The air temperature varied between –19.8 and 2.3°C. At 06:00 UTC the temperature on the surface of the snowpack was –22.9°C. Next, the clear sky cases of the melt season were studied.

Table 3. SL501 UV albedo of Arctic snow at Sodankylä for midday SZA<60° in April 2007. Both the date and number of the day are given. The column of diurnal decline in albedo refers to temporary decline soon after midday (approx. duration), whereas asymmetric decline suggests a decline from morning towards afternoon.

Date	Snow conditions	Cloudiness	Albedo minimum and maximum	Albedo average	Diurnal decline
10.4. (100)	Accumulation period	Almost clear	0.64–0.67 (stable, slightly highest at midday)	0.66	NO
11.4. (101)	Accumulation period	Almost overcast	0.72–0.81 (stable, temporary high values due to snow fall)	0.74	NO
12.4 (102)	Snow melt period starts	Variable	0.66–0.70 (stable, slight indication of diurnal decline)	0.69	NO
13.4. (103)	Melt	Variable	0.66–0.68	0.67	NO
14.4. (104)	Melt	Variable	0.61–0.65 (slight indication of diurnal decline)	0.63	NO
15.4. (105)	Melt	Almost clear	0.55–0.60	0.59	YES (60 min)
16.4. (106)	Rapid melt	Variable	0.56–0.60	0.58	YES (20 min)
17.4. (107)	Rapid melt	Variable	0.54–0.60	0.57	YES (60 min)
18.4. (108)	Rapid melt	Almost clear	0.54–0.60	0.58	YES (100 min)
19.4. (109)	Rapid melt	Variable	0.56–0.63	0.60	YES (60 min)
20.4. (110)	Rapid melt	Variable	0.56–0.62	0.59	YES (60 min)
21.4. (111)	Melt	Variable	0.58–0.61 (stable or slightly lowest at midday)	0.59	NO
22.4. (112)	Melt	Almost clear	0.55–0.60	0.56	YES (100 min)
23.4. (113)	Melt	Almost overcast	0.57–0.61	0.58	NO
24.4. (114)	Melt	Variable	0.51–0.58 (suggesting asymmetric decline)	0.55	YES (80 min)
25.4. (115)	Melt	Variable	0.50–0.54	0.52	YES (80 min)
26.4. (116)	Melt	Variable	0.51–0.52	0.51	NO
27.4. (117)	Melt	Variable	0.46–0.49 (suggesting asymmetric decline)	0.47	NO
28.4. (118)	Melt	Variable	0.46–0.50 (stable or slightly lowest at midday)	0.47	NO
29.4. (119)	Melt	Variable	0.44–0.5 (stable or slightly lowest at midday)	0.47	NO
30.4. (120)	Melt	Variable	0.44–0.46	0.45	NO

4.1.2 Diurnal change in albedo during melting

The second, almost clear sky case of 15 April (day 105) occurred at the very beginning of the snow melt period. During the measurements from 09:00 to 12:00 UTC with SZA 56–60°, the albedo of the snow unexpectedly decreased by 0.05 from 0.6 to 0.55, and then recovered (Fig. 8). The drop in albedo happened soon after solar midday.

The next two almost clear sky cases came in the middle of the melting season, when almost 1/3 of the accumulated snow had melted. On 18 April (day 108), a similar behaviour in snow albedo occurred: a clear change from 0.6 to 0.55 and a recovery back to 0.6. On 22 April (day 112), the same occurred again, but this time the albedo varied at a slightly lower level, changing from 0.58 to 0.53.

Hence, in all three cases at the snow melt period a slight drop in the general albedo level (Fig. 8), asymmetrical to the solar zenith angle, was observed to be superimposed on the general albedo level.

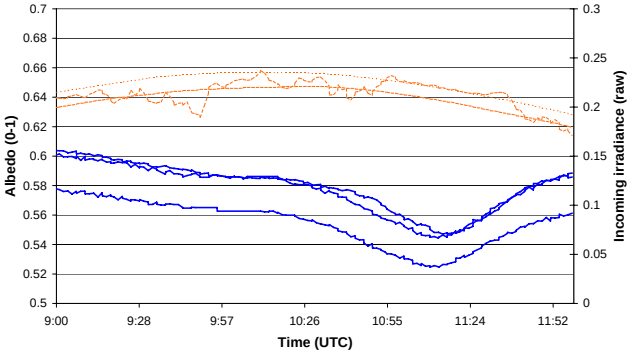

Fig. 8. Diurnal decrease of albedo under clear sky cases of 15, 18 and 22 April (days 105, 108, 112), marked with the solid blue lines. The incoming irradiances are marked with the dashed orange lines.

For a more detailed study, data on temperature, incoming irradiance, and multichannel NILU-UV albedo in the UVA and UVB channels were available:

– 15 April (day 105): the snow depth was 58 cm, and the measured air temperatures were between 2.2–12.2°C. At 06:00 UTC Tmin on the ground was close to zero (0.5°C), and in the next morning it was below the zero (–4.1°C); during that next day the snow depth decreased by 3 cm, with a very thick surface layer (35 cm) and large snow grain size (2.5 mm), indicating a major snow metamorphosis. In the NILU-UV data, both the UVA and UVB albedo decreased, similarily to SL501 albedo.

– 18 April (day 108): air temperature was from –7.8 to 4.2°C, and the snow depth was 45 cm. The next morning, Tmin on of the ground was –4.9°C. In the NILU-UV albedo data, both the UVA and UVB decreased, too. Two days later, a snow grain size of 2.0 mm was measured, while the surface layer depth was 17 cm, both indicating snow metamorphosis and melting continuing intensively.

– 22 April (day 112): air temperatures ranged from –9.9 to 7.9°C, and snow depth was 42 cm. In the NILU-UV data, both UVA and UVB albedo decreased again.

Therefore, we know that the temperature on the snow surface was below zero in the next morning at 06:00 UTC in two cases, but in the first case did temperature remain slightly above zero (0.5°C). The largest grain size of 2.5 mm was measured in this case, too. In all cases, the NILU-UV data confirmed the unexpected discovery using SL501 data: a diurnal change of UV albedo asymmetrically to solar midday was detected using two independent measurement devices.

4.2 UV albedo under variable cloudiness

4.2.1 Stable albedo during accumulating snow

The smallest grain sizes of 0.2–0.3 mm, indicating new snow or snow below-zero conditions during the period of accumulating snow, were observed on four days. Those days were: 20 March; 3, 5, and 10 April (days 79, 93, 95, and 100). The most reliable calibration is for 10 April, which was presented with the clear sky results. The next most reliable cases were on the 3 April: a midday, and stable, albedo of 0.68. On the 5 April the albedo was 0.72, and stable. These cases thus confirm the clear sky case: during the snow accumulation period, the albedo remains stable, increasing slightly, if at all, increasing in the midday period.

4.2.2 Diurnal albedo of melting snow under variable cloudiness

There were two days on which the maximum snow grain size of 2.5 mm in the surface layer, i.e., 16 April and 8 May (days 106 and 128), was measured. On 17 April (day 107) the grain size was measured to be 2 mm, with a 17 cm top layer.

On the basis of the AWS snow depth measurement, the snow pack decreased monotonically since 12 April (day 102). We therefore assume the period of rapid melting, with the largest grain sizes, to have taken place during, at least, the days of 16–20 April (days 106–110). 8 May (day 128) is at the end of the measurement period with the snow partly melted, revealing the ground, too. For this reason these data were not included the cases presented here:

– 16 April (day 106): the thickness of the surface layer was 35 cm, whereas during the three earlier measurements, during the whole accumulation period, it had varied from 1 to 6 cm. Hence, a major change in the snow, with a deep metamorphosized and homogenized surface layer, took place on that day. The cloudiness was highly variable, yet a drop in the SL501 albedo after midday from 0.6 to 0.55 took place.

– 17 April (day107): the snow depth was 50 cm at 06:00 UTC, and 46 cm at 18:00 UTC. The next day it was 45 cm. From this we can conclude that conditions similar to those on the clear sky day of 15 April (day 105), continued on days 106 and 107, despite the variable cloudiness. The SL501 albedo dropped from 0.6 to 0.55 after midday, and then recovered.

– 19 April (day 109): the results showed a similar diurnal decrease in albedo, too.

– 20 April (day 110): the cloudiness was highly variable, but the SL501 albedo decreased from approx. 0.6 to 0.55, as had been found in the clear sky cases earlier presented.

Hence, these cases with variable cloudiness confirm the clear sky SL501 cases during the melting season: an albedo slightly decreasing by 0.05 soon after midday, and then recovering after that.

4.3 Albedo before and after the period of diurnal change

The period of variable albedo began on the 15 April, and ended on 25 April (days 105–115). The cases before and after these dates show a flat albedo signal (Table 3). Prior to the diurnal albedo change, a flat signal of $A>0.6$ was detected. On the basis of the snow depth data, this was the period before the snow melt. Following the variable diurnal albedo, there was a diurnally-stable midday albedo, of $A<0.5$. These results would suggest that, after a drop in the albedo to a level of 0.5, the diurnal change in the albedo disappears, possibly signaling the end of some stage in the melting process.

4.4 Average daily UV albedo of melting snow

The midday erythemally weighted UV albedo ranged from 0.6 to 0.8 in the accumulation period, and from 0.5 to 0.7

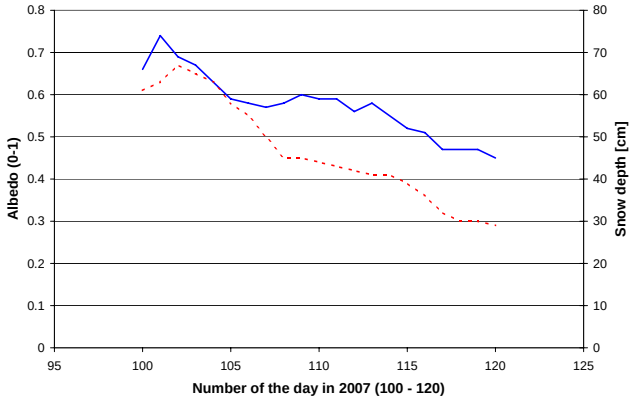

Fig. 9. The measured snow depth (dashed red line) and the measured albedo (solid blue line). Average of snow UV albedo for midday and snow depth for each day during melt season from 10 to 30 April (days 100–120) in spring 2007.

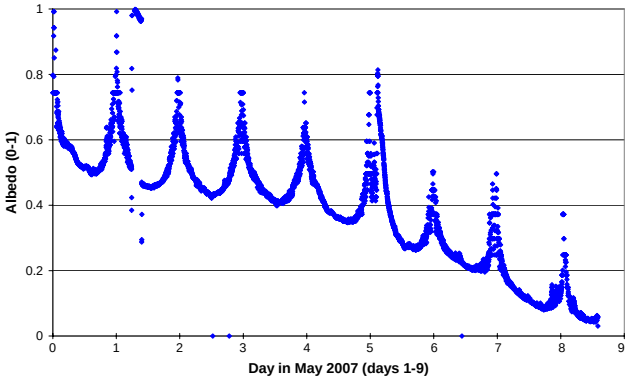

Fig. 10. May albedo data with the U-shape appearing each day. Only cases SZA<85° for each day from 1 to 9 May (days 121–129) shown here.

during melting. The averaged daily UV albedo of snow for 56<SZA<60 degrees during the melt was a second-order polynomial as a function of snow height:

$$A = -6\mathrm{E} - 05h_s^2 + 0.0114h_s + 0.1809 \quad (4)$$

where h_s is the snow height [cm]. This formulation, with r^2=0.86, is adjusted for the melt period only (data of days 100–120, Fig. 9).

4.5 Long term variation in SL501 UV albedo

Studying the time series of the continuous 1-minute albedo data, the SZA-dependency (U-dependency) of the differences between the responses of the sensors is evident (Fig. 10), as well as the occurrence of evening and night-time with no incoming irradiance. On closer inspection, when the midday data with SZA 56–60° are used, the albedo signal is quite flat (e.g., Fig. 7).

An increase in albedo from 0.72 to 0.81 was detected on 11 April (day 101), possibly due to new snow (as evidenced from the AWS data for the same time), but further study is beyond the scope of the present work. More detailed study would require a detailed analysis focusing on the AWS rain data.

The SL501 midday albedo results for Arctic snow, can be divided into two groups: an albedo of 0.6–0.8 between 22 March–14 April (days 81–104) (the accumulation period), and an albedo of 0.4–0.6 between 15 April–3 May (days 105–123) (snow melt). These data were calibrated by using different empirical calibration factors for cases SZA<60° and for SZA>60°. In studying the hypothetical effect of using the March coefficients (midday SZA>60°) for May data, an error<6% was caluculated for 09:00–12:00 UTC. The use of different coefficients for the prevailing SZA conditions, as presented earlier, reduced this error in the long term data.

The albedo of snow was recorded to lower little by little as the snow melted (Fig. 10). The results would also suggest a possible SZA asymmetry in snow albedo (Table 3). The calibration procedures presented in this study have no effect on this finding, as it is a question of asymmetry according to noon: a SZA correction would produce SZA symmetric data if the prevailing conditions had not changed between noon and afternoon. Yet, to study this SZA asymmetry further would require knowledge on the factors affecting the SZA correction in the data (such as the ratio of direct-to-diffuse irradiance). After the beginning of May, the albedo results were characterized more by the amount of ground visible, than by the actual albedo properties of the snow.

5 Discussion

5.1 About errors and uncertainties

Here, use was made of erythemal UV albedo measurements by broadband SL501 radiometers with similar spectral responses, thus resulting in errors of less than 1% due to differences in the sensors (WMO, 1996). According to Hülsen and Gröbner (2007), the typical total uncertainty for SL501 instruments is from 1.7 to 4.3 %. The calibration of the sensors was made before (in 2005 and 2006) and after (2007) the albedo measurements. Prior to the albedo measurements, the spectral and cosine responses of the sensors had been determined to be similar, as presented in Figs. 1 and 2. In the albedo data, the SZA-dependency (U-shape) became evident. We suspected this to be due to changed spectral response. This was confirmed in the post-calibration measurements (Fig. 4). On the basis of our experience, the spectral responses of SL501 sensors may change in time, and therefore the responses should be determined on a regular basis, preferably every year or every second year.

Basically, a drift in a sensor response might be nonlinear, either momentary or lasting, or even occasionally due

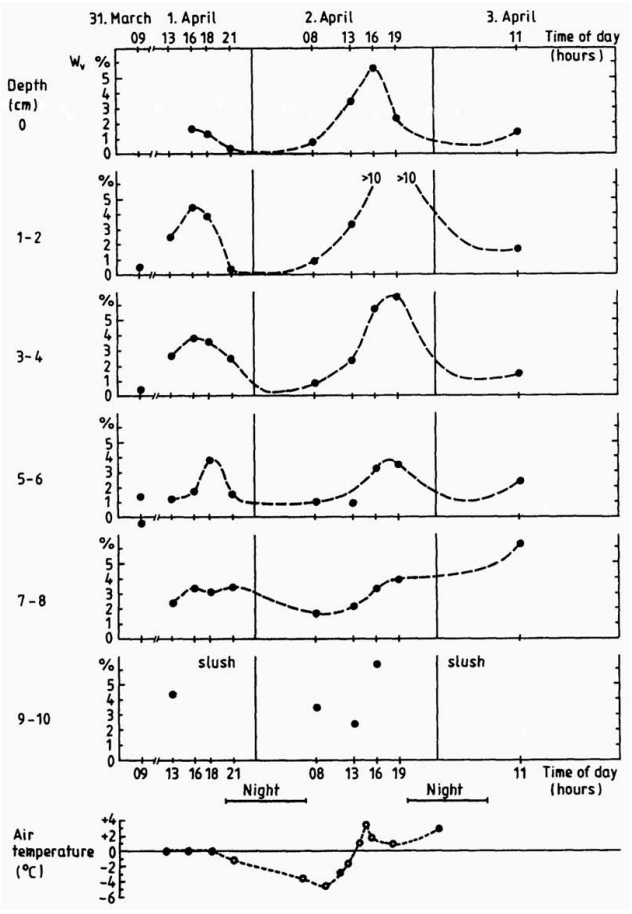

Fig. 11. Measured diurnal variation of liquid water content at different depth levels of snow pack.

to environmental conditions, such as the internal humidity of the sensor, temperature, total ozone, etc. Here, the problem was solved by empirical calibrations, as described, and by using only the data within a SZA-range of 56–60 degrees for the analysis. Thereafter, the error in the data due to the sensors can be determined on the basis of the post-calibration measurements (Fig. 3): within an SZA of 56–60°, the SZA dependency, i.e., the U-shape due to difference in the spectral responses of the sensors, caused an error of less than 3%. The U-shape in the results might also be partly due to the different components the upward and downward radiometers see (for downward looking sensor the diffuse and specular, while for the upward sensor the direct and diffuse). Even if both had identical spectral and angular responses, the errors induced by the combination of imperfect response functions and radiance distributions may be different for the two radiometer orientation. Also, the different orientations of the radiometers might possibly alter the internal temperature and thus affect the responsitivity.

With these empirically calibrated data, any possible dependency of albedo on solar zenith angle could only be compared for similar conditions of cloudiness and solar zenith angles. The empirical calibration provides a direct comparison of the two radiometer readings but then only a smaller SZA range is utilized and the SZA influence on the albedo remains unresolved. On the other hand, any albedo asymmetry close to midday could be reliably studied for SZA 56–60° without introducing any additional uncertainty or error in the data due to a simplified SZA correction. For example, a SZA and ozone dependent calibration factor can not correct the data unless a proper spectral reponse funtion of the sensor is used. An example of such an error (an outlier) possibly introduced by a simple SZA correction in the albedo data is presented in Wuttke et al. (2006). On the basis of our experience, an optimal 1-min SZA correction, for both the upward and downward broadband sensor independently, would require knowledge on the spectral and cosine response functions, temperature correction functions, and 1-minute data on the radiation distribution, and the ratio of the diffuse-to-direct irradiance affected by clouds, ozone, aerosols, albedo and SZA. Hence, the general measurement equation requires a thorough characterization of the two radiometers but may then remove the most SZA dependent artefacts. How ever, the problem of changed spectral response remains. According to our experience, if applying this equation, the spectral responses are to be determined prior and after the measurements.

5.2 Diurnal variations in the albedo

An unexpected diurnal change in UV albedo, measured by the SL501 sensors, was detected during the melt period at SZA $<60°$. The albedo decreased by approx. 0.05 soon after midday and then recovered to the same, or almost the same, level. If this diurnal variation in albedo were to be due to any shadowing effects, rather than the properties of snow, the shadowing would be best seen under clear sky conditions, and not in cloudy situations. Here the diurnal change was evident for all states of sky. Furthermore, as the sensor facing upward was at the same height as the sensor measuring reflected radiation, any shadowing would necessarily be evident in the signal of the incoming irradiance at some time during the day (although not necessarily at the exactly same time as the downward sensor recorded the reflected radiation from the shadowed surface). The incoming irradiance did not indicate any such shadowing (Fig. 8). Also, when the site for the albedo measurements was chosen, the horizon towards the South was selected to be without shadowing. The pole and the frame supporting the sensors were also placed to the North to avoid shadows. Finally, the same diurnal decrease was evident in the data of the NILU-UV radiometer measuring the upwelling radiation close to the SL501.

Our findings on UV albedo of natural melting snow are in accordance with the speculations presented by Wiscombe

and Warren (1980). They explain that snow albedo decrease due to liquid water content increase follows from the fact that liquid water replaces air between ice grains. As the refractive index of liquid water is close to ice for wl<5000 nm, the replacement of air by liquid water between ice grains could increase the effective grain size.

Furthermore, the results of diurnal variation of liquid water content at various snow layers (Fig. 11) by one of the authors (M. Toikka) suggest that the temperature rise increases the liquid water content first on the surface layer of the snowpack. Then, as the temperature drops toward evening and night, the liquid water falls into deeper layers. Thus, liquid water on the snow surface, as well as the effective grain size due to liquid water, would increase only temporarily. When the temperatures drop, most of the liquid water is no longer in the surface layer, but in the layers below. Thus, these diurnal results of the liquid water in snow anticorrelate with the diurnal albedo results, offering empirical explanation to our albedo observations. Earlier, Kuusisto (1984) has also stated that the thick snow cover in northern Finland starts to release water from surface layers through percolation channels, while the deeper layers of the cover are still relatively unmetamorphosized. Opposite to this, in southern Finland, the thin snow cover is quickly metamorphosized all the way to the ground surface.

Similar results on diurnal decline of albedo were observed by Pirazzini in the Antarctica (personal communication, 2007), although not reported in the article by Pirazzini (2004). The same diurnal decline was observed by them in Arctic conditions, too (Pirazzini et al., 2006). In the Antarctic conditions, their observation for the diurnal decline was later in the afternoon. Earlier, a minimum albedo has been detected by McGuffie and Henderson-Sellers (1985) in Canada, too. They suggested the albedo decrease to be due to snow grain metamorphosis caused by heating of the surface.

According to Grenfell et al. (1994) the albedo of snow depends on its physical properties, and varies according to wavelength. Here, the spectral distribution of the snow albedo between UVA and UVB could be studied on the basis of a multiband filterradiometer facing downwards, and another upward MBFR radiometer nearby. These complementary results confirmed the findings of diurnal variability in the UVB albedo.

5.3 Asymmetric albedo

In the current study some indication on the asymmetric UV albedo was observed, too (Table 4). Also, McGuffie and Henderson-Sellers (1985) have reported of diurnal hysteresis of snow albedo, i.e. that the albedo is different for the same solar elevation angle at different times of day. They suggest the variation should be attributed to the diurnal deposition and evaporation of a hoar-frost coating on the snow surface. Pirazzini (2004) and Wuttke et al. (2006) have recorded more recently albedo results in the Antarctic sites with several instruments, which are opposite to the ones predeicted by theory. They both found a decline of albedo for increasing SZA. A possible levelling error was not consired the source for this observed diurnal cycle. Wuttke et al. (2006) speculate the reason for this opposite dependence of albedo on SZA to be rather due to changing snow conditions due to the steady solar insolation. Pirazzini et al. (2006) found similar results in Arctic conditions, too. Earlier, McKenzie et al. (1996) speculated that their UV albedo measurements of long grass (no snow) showing slightly higher albedos in the afternoon than in the morning might be due to either various error sources (e.g., leveling, angledependent reflections) or real changes in the surface, (e.g., morning dew evaporating or light dependent plant physiology). Hence, it is essential to understand and separate all the factors affaecting the albedo results.

5.4 Polar snow and albedo

When Arctic and Antarctic albedo are compared, the reasons to differences might be several, in addition to snow grain size and amount of impurities; e.g., Hansen and Nazarenko (2004) have studied soot climate forcing in the Arctic via snow and ice albedos. If we consider other possible contributors to differences in albedo, these might be due to, e.g., snow grain shape and topography. Differences in precipitation snow grain shapes might, in principle, be due to differences, e.g., in the atmospheric moisture (Antarctic air is known to be dryer than the Arctic atmosphere), temperature (Antarctic atmosphere is colder than Arctic, and sometimes stratospheric air masses reach down into the troposphere there), and aerosol amounts (cleaner Antarctic air). Also, although the measurement area is quite flat, the local albedo may be affected by the topography.The irradiance ratios are influenced not only by the local snow albedo underneath the radiometers, but also the combination of low-albedo and high-albedo surfaces within a larger radius. E.g., Kylling et al. (2000) have studied the effect of inhomogeneous surfaces on the effective albedo. However, although the local albedo is affected by the regional albedo, our measurements at a height of 2 m may be considered to represent local albedo. Furthermore, a term “effective local albedo”, for instance, could be more descriptive for the albedo quantity derived in our study. The critical question is whether the downwelling radiation field on the snow surrounding the observation point (i.e., in the area where the observed $F(\uparrow)$ originates), differs systematically from $F(\downarrow)$ at the observation point. If not, $F(\uparrow/\downarrow)$ should be an accurate estimate of the local albedo. Additionally the snow albedo may have a specular component (Mie scattering), giving rise to a SZA dependent variation. At high SZAs, the Mie scattered photons scattered forward into the snowpack have a greater chance of escaping the snow and still reach the downward-looking sensor. This could partly explain the diurnal U-shape of the albedo. Hence, the specular component may have an important role.

During the winter of 2006/2007, permanent snow fell in Sodankylä in the middle of October, but almost all the snow melted at the end of November (Kontu et al., 2007). Snow density during the winter months was determined to be from 0.18 to 0.21 g/cm^3 (Kontu et al., 2007). In addition to the temperature, other environmental factors, like rainfall, wind, humidity, cloudiness, as well as the properties of the snow and the ground under the snow, affect the process of snow melt. On the basis of AWS data on snow depth, 12 April (day 102) was the date after which the snow amount only decreased from one day to the next. Hence, these data are in accordance with the start of diurnal albedo change detected from 15 until 25 April (days 105–115). The prior and subsequent albedo was stable.

6 Conclusions

For snow the grain size has been reported to vary generally by less than 50% on the topmost 10–20 cm of snow (Warren and Wiscombe, 1980). We found that in the Arctic conditions of Sodankylä, belonging to the global snow class of Taiga snow (Sturm et al., 1995), the grain sizes of the top layer varied from 0.2 to 2.5 mm, containing variation by 125%. Thus the variability in grain size of the Arctic snow in Finland, and the maximum grain sizes were found to be extreme.

In a literature review presented in Warren and Wiscombe (1980) for their albedo model, it was found that some papers reported the albedo to increase with solar zenith angle. We found a slight increase at midday during the accumulation period with small grain size. This could possibly be physically explained by an increase in the specular component at midday compared to morning or afternoon. The midday increase would then be the bigger the smaller the grain size.

In summary, our results suggest:

- a high and stable midday albedo for SZA 56–60° during the snow accumulation period; albedo maximum in solar midday during accumulation period in clear sky and under variable cloudiness
- possibly UV albedo asymmetric to solar zenith angles
- a diurnal change of 0.05 in albedo during the melt period, in cases of clear sky and variable cloudiness with SZA 56–60°
- a little by little decrease in the general abedo level with the melting of snow
- a stable lower albedo at the end of the melt period.

With the help of ancillary data on temperature, grain size and snow depth, these are explained by a high albedo induced by a small grain size during accumulation time, and a diurnal change in albedo by snow grain metamorphosis caused by heating of the surface, melting some of the snow to liquid water, and the metamorphosis ceasing by the end of the melt period. These findings were made possible only by continuous high temporal resolution measurements, and would not have been found by measurement campaigns.

The advantages of snow albedo measurements in Finland are the facts that here i) the snow cover melts every year, and ii) we have five out of the six global snow classes (Sturm et al., 1995), only the alpine snow missing, and iii) the topography in Finland is flat, thus favorable to albedo studies, iv) clean snow can be found in the remote areas of the Finnish Lapland, vi) the snow grain size of the top layer varies greatly from small to extremely big grain sizes of 2.5 mm. In the future, we intend to continue ground-based UV albedo measurements under these conditions in Finland, and comparisons are planned to extend to Arctic-Antarctic, and between UV and broadband albedo. The liquid water content of the top layer of the snow from midday for two hours forward at intervals of approx. half an hour or even less should be measured in the melt period together with continuous high temporal resolution (1-min) albedo measurements and the ancillary data as presented here. Possibly some other parameters may also be included (including spectral albedo), or the temporal resolution of the parameters may be improved to study the diurnal decrease and the possible asymmetry. Wiscombe and Warren (1980) have reported that only a small number of albedo models had been put forward prior to their model, reflecting the lack of high-quality data against which to check such a model, and the fact that some of the data are contradictory. The albedo model introduced in their paper is in use in the commonly-applied radiative transfer (RT) model Libradtran (Mayer and Kylling, 2005), and currently highly referred to. Using our empirical data, a UV albedo parametrization for Arctic snow during accumulation and melt time periods could be elaborated, and the existing albedo models verified.

Acknowledgements. The authors are grateful to A. Aarva, H. Suokanerva, S. Suopajärvi, V. Postila, and P. Koivula for their help with operation of the SL501 sensors. The Academy of Finland has given financial support for this work (FARPOCC-project).

Edited by: M. Blumthaler

References

Arola, A., Kaurola, J., Koskinen, L., Tanskanen, A., Tikkanen, T., Taalas, P., Herman, J.R., Krotkov, N., and Fioletov, V.: A new approach to estimating the albedo for snow-covered surfaces in the satellite UV method, J. Geophys. Res., 108(D17), 4531, doi:10.1029/2003JD003492, 2003.

Bais, A. F. and Dan Lubin, D.: Chapter 7: Surface Ultraviolet Radiation: Past, Present, and Future, In: WMO: Scientific Assessment of Ozone Depletion: 2006, World Meteorological Organization Global Ozone Research and Monitoring Project-Report No. 50, Final Release: February, 2007.

Bernhard, G. and Seckmeyer, G.: Uncertainty of measurements of spectral solar UV irradiance, J. Geophys. Res. 104(D12), 14 321–14 345, 1999.

Blumthaler, M. and Ambach, W.: Solar UVAlbedo of various surfaces, Photochemistry and Photobiology, 48(1), 85–88, 1988.

Bony, S. Colman, T., Kattsov, V. M., Allan, R. P. Bretherton, C. S., Dufresne, J.-L., Hall, A., Hallegatte, S., Holland, M. M., Ingram, W., Randall, D. A., Soden, B. J., Tselioudis, G., and Webb, M. J.: REVIEW ARTICLE, How Well Do We Understand and Evaluate Climate Change Feedback Processes?, J. Climate, 19, 3445–3482, 2006.

Forster, P., Ramaswamy, V., Artaxo, P., Berntsen, T., Betts, R., Fahey, D. W., Haywood, J., Lean, J., Lowe, D. C., Myhre, G., Nganga, J., Prinn, R., Raga, G., Schulz, M., and Dorland, J. V.: Changes in Atmospheric Constituents and in Radiative Forcing, in: Climate Change 2007: The Physical Science Basis. Contribution of Working Group I to the Fourth Assessment Report of the Intergovernmental Panel on Climate Change edited by: Solomon, S., Qin, D., Manning, M., Chen, Z., Marquis, M., Averyt, K. B., Tignor, M., and Miller, H. L., Cambridge University Press, Cambridge, United Kingdom and New York, NY, USA, 2007.

Grenfell, T. C., Warren, S. G., and Mullen, P. C.: Reflection of solar radiation by the Antarctic snow surface at ultraviolet, visible, and near-infrared wavelengths, J. Geophys. Res., 99(D9), 18 669–18 684, 1994.

Hansen, J. and Nazarenko, L.: Soot climate forcing via snow and ice albedos, Proc. Natl. Acad. Sci., 101, 423–428, doi:10.1073/pnas.2237157100, 2004.

Hoiskar, B. K., Haugen, R., Danielsen, T., Kylling, A., Edvardsen, K., Dahlback, A., Johnsen, B., Blumthaler, M., and Schreder, J.: Multichannel Moderate-Bandwidth Filter Instrument For Measurement Of The Ozone-Column Amount, Cloud Transmittance, And Ultraviolet Dose Rates, Appl. Optics, 42, 3472–3479, 2003.

Hülsen, G. and Gröbner, J.: Characterization and calibration of ultraviolet broadband radiometers measuring erythemally weighted irradiance, Appl. Optics, 46(23), 5877–5886, 2007.

IPCC: Climate Change 2007 – The Physical Science Basis, Contribution of Working Group I to the Fourth Assessment Report of the IPCC, (ISBN 978 0521 88009-1 Hardback; 978 0521 70596-7 Paperback), http://www.ipcc.ch/ipccreports/ar4-wg1.htm, 2007.

Kontu, A., Pulliainen, J., Heikkinen, P., Suokanerva H., and Takala, M.: Validation of Microwave Emission Models by Simulating AMSR-E Brightness Temperature Data from Ground-based Observations, Proc. 2007 IGARSS, Barcelona, Spain, 2007.

Kuusisto, E.: Snow accumulation and snowmelt in Finland. Helsinki, Publications of the water Research Institute 55, ISBN 951-46-7494-4, 149 p., 1984.

Kylling, A., Persen, T., Mayer, B., and Svenøe, T.: Determination of an effective spectral surface albedo from ground-based global and direct UV irradiance measurements, J. Geophys. Res., 105(D4), 4949–4959, 2000.

Madronich, S.: Environmental UV Photobiology, Chap. 1, The Atmosphere and UVB Radiation at Ground level. Plenum Press, New York, 1993.

Mayer, B. and Kylling, A.: Technical note: The libRadtran software package for radiative transfer calculations – description and examples of use, Atmos. Chem. Phys., 5, 1855–1877, 2005, http://www.atmos-chem-phys.net/5/1855/2005/.

McGuffie, K. and Henderson-Sellers, A.: The diurnal hysteresis of snow albedo, J. Glaciol., 31(108), 188–189, 1985.

McKenzie, R. L., Kotcamp, M., and Ireland, W.: Upwelling UV spectral irradiances and surface albedo measurements at Lauder, New Zealand, Geophys. Res. Lett., 23(14), 1757–1760, 1996.

Meinander, O., Kazadzis, S., Blumthaler, M., Ylianttila, L., Johnsen, B., Lakkala, K., Koskela, T., and Josefsson, W.: Diurnal discrepancies in spectral solar UV radiation measurements, Appl. Opt. 45, 5346–5357, 2006.

Perovich, D. K., Grenfell, T. C., Light, B., and Hobbs, P. V.: Seasonal evolution of the albedo of multiyear Arctic sea ice, J. Geophys. Res., 107(C10), 8044, doi:10.1029/2000JC000438, 2002.

Pirazzini, R.: Surface albedo measurements over Antarctic sites in summer, J. Geophys. Res., 109, D20118, doi:10.1029/2004JD004617, 2004.

Pirazzini, R., Vihma, T., Granskog, M., and Cheng, B.: Surface albedo measurements over sea ice in the Baltic Sea during the spring snowmelt period, Ann. Glaciol., 44, 7–14, 2006.

Smolskaia, I., Nunez, M., and Kelvin, M.: Measurements of Erythemal Irradiance near Davis Station, Antarctica: Effect of. Inhomegeneous Surface Albedo, Geophys. Res. Lett., 26, 1381–1384, 1999.

Sturm, M., Holmgren, J., and Liston, G. E.: A seasonal snow cover classification system for local to global applications, J. Clim., 8, 1261–1283, 1995.

Tanskanen, A. and Manninen, T.: Effective UV surface albedo of seasonally snow-covered lands, Atmos. Chem. Phys., 7, 2759–2764, 2007, http://www.atmos-chem-phys.net/7/2759/2007/.

UNEP: Environmental Effects of Ozone Depletion: 2002, Assessment, United Nations Environment Programme. ISBN 92-807-2312-X, http://www.unep.org/OZONE/pdf/eeap-report2002.pdf, 2002,

Warren, S. G. and Wiscombe, W. J.: A model for the spectral albedo of snow. II: Snow containing atmospheric aerosols, J. Atmos. Sci., 37, 2734–2745, 1980.

Weatherhead, B., Tanskanen, A., Stevermer, A., Andersen, S., Arola, A., Austin, J., Bernhard, G., Browman, H., Fioletov, V., Grewe, V., Herman, J., Josefsson, W., Kylling, A., Kyrö, E., Lindfors, A., Shindell, D., Taalas, P., and Tarasick, D.: Chapter 5: Ozone and Ultraviolet Radiation. ACIA 2005. Arctic Climate Impact Assessment. Cambridge University Press, 1042, 151–182, 2005.

Webb, A., Gröbner, J., and Blumthaler, M.: A practical guide to operating broadband instruments measuring erythemally weighted irradiance, WMO SAG UV, COST-726, ISBN 92-898-0032-1, 2006.

Wiscombe, W. J. and Warren, S. G.: A model for the spectral albedo of snow. I: Pure snow, J. Atmos. Sci., 37, 2712–2733, 1980.

WMO: WMO GAW report 120. WMO-UMAP Workshop on Broad-Band UV Radiometers, Garmisch-Partenkirchen, Germany, 22–23 April 1996, WMO TD No. 894, 1996.

Wuttke, S., Seckmeyer, G., and König-Langlo, G.: Measurements of spectral snow albedo at Neumayer, Antarctica, Ann. Geophys., 24, 7–21, 2006